

Optimal cavity design for minimizing errors in cavity-QED-based atom-photon entangling gates with finite temporal duration

Takeru Utsugi,^{1,*} Rui Asaoka,^{2,†} Yuuki Tokunaga,² and Takao Aoki¹

¹*Department of Applied Physics, Waseda University,
3-4-1 Okubo, Shinjuku-ku, Tokyo 169-8555, Japan*

²*Computer & Data Science Laboratories, NTT Corporation, Musashino, Tokyo 180-8585, Japan*
(Dated: November 9, 2022)

We investigate atom-photon entangling gates based on cavity quantum electrodynamics (QED) for a finite photon-pulse duration, where not only the photon loss but also the temporal mode-mismatch of the photon pulse becomes a severe source of error. We analytically derive relations between cavity parameters, including transmittance, length, and effective cross-sectional area of the cavity, that minimize both the photon loss probability and the error rate due to temporal mode-mismatch by taking it into account as state-dependent pulse delay. We also investigate the effects of pulse distortion using numerical simulations for the case of short pulse duration.

Atom-photon gates are key components for universal quantum computation [1] based on cavity quantum electrodynamics (cQED) [2], as these gates can be used to implement both atom-atom gates [3–6] and photon-photon gates [7, 8], which are expected to enable the construction of scalable distributed quantum computation systems [2]. Recently, one of the entangling gates, a controlled phase flip (CPF) gate between atomic and photonic qubits in cQED systems, has been experimentally demonstrated [5, 6, 8–10].

Previous theoretical investigations for atom-photon CPF gates have shown that the error probabilities are characterized by the internal cooperativity parameter C_{in} in the limit where the input-photon pulse duration is infinite [11–13]. Since C_{in} is proportional to \mathcal{F}/\mathcal{A} in typical cavities, where \mathcal{F} is the finesse and \mathcal{A} is the mode area [2, 14, 15], in the long pulse limit, high-finesse cavities with small mode areas are required to suppress errors [16–18]. On the other hand, we have previously shown that the error probabilities in the CPF gate cannot be characterized only by C_{in} when the photon pulse is of a finite duration [13]. This result suggests that the optimal cavity design should be reconsidered for finite pulse duration, which is required to achieve fast gate operation, and represents a more natural experimental description.

In this Letter, we investigate the optimal cavity design for cQED-based CPF gates. In the case of finite pulse duration, the atom-photon gates have two severe error sources: the photon loss and the temporal mode-mismatch of the output photon pulse. Here, the dominant effect of temporal mode-mismatch can be considered as pulse delay. In this approximation, we derive the relations between cavity parameters, including transmittance, length, and effective cross-sectional area of the cavity, that minimize both the photon loss probability and the error rate due to the pulse delay. It is especially worth noting that the cavity length has an optimal value

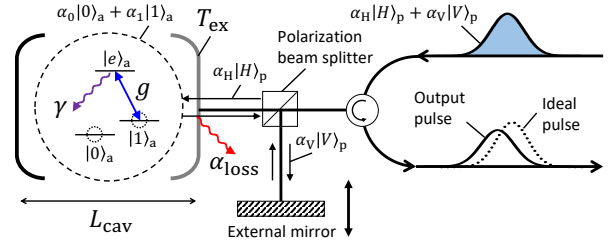


FIG. 1. Schematic of the atom-photon CPF gate. The photon carries qubit information represented by the polarization states $\alpha_H|H\rangle_p + \alpha_V|V\rangle_p$, and the two ground states of the trapped three-level atom in the cavity represent an atomic qubit $\alpha_0|0\rangle_a + \alpha_1|1\rangle_a$. The transition between $|1\rangle_a$ and $|e\rangle_a$ in the atom is resonant with the cavity. Through the polarizing beamsplitter, the input photon having horizontal (vertical) polarization, $|H\rangle_p$ ($|V\rangle_p$), is directed to the one-sided cavity (the external mirror). The cavity length L_{cav} , the cavity transmittance T_{ex} , and the position of the external mirror are adjustable. The notation g is the atom-cavity coupling constant, γ is the atomic polarization decay rate, and α_{loss} is the roundtrip loss rate of the cavity.

in our analysis, which is not the case for the long pulse limit as C_{in} is independent of the cavity length. We also perform numerical simulations of the dynamics of the cQED system and discuss the effect of pulse distortion when the pulse is short.

Figure 1 shows a setup to realize the atom-photon CPF gate [9–11]. An atom in a one-sided cavity has an excited state $|e\rangle_a$, and ground states $|0\rangle_a$ and $|1\rangle_a$, which represent qubit bases. The transition between $|1\rangle_a$ and $|e\rangle_a$ is resonant with the cavity. A photon qubit is represented by its polarization $|H\rangle_p$ and $|V\rangle_p$. The initial state of the entire system is then written as

$$|\Psi_{\text{in}}\rangle = (\alpha_0|0\rangle_a + \alpha_1|1\rangle_a) \otimes (\alpha_H|H\rangle_p + \alpha_V|V\rangle_p), \quad (1)$$

where α_i ($i \in \{0, 1, H, V\}$) are complex amplitudes.

An input single-photon pulse is split using a polarizing beamsplitter so that only one polarization is incident on the cavity (we choose $|H\rangle_p$ here).

* utsugitakeru@akane.waseda.jp

† rui.asaoka.st@hco.ntt.co.jp

The other component is reflected by an external mirror. We describe the output state after the atom-photon interaction via the cavity mode as

$$|\Psi_{\text{out}}\rangle = L_0\alpha_0\alpha_H|0H\rangle + \alpha_0\alpha_V|0V\rangle \\ + L_1\alpha_1\alpha_H|1H\rangle + \alpha_1\alpha_V|1V\rangle, \quad (2)$$

where $|jk\rangle = |j\rangle_a \otimes |k\rangle_p$ ($j \in \{0, 1\}, k \in \{H, V\}$). When $L_0 = -1$ and $L_1 = 1$, the ideal CPF gate operation is realized.

Denoting the annihilation (creation) operators inside and outside of the cavity as $a_c (a_c^\dagger)$ and $a_p (a_p^\dagger)$, the Hamiltonian of the cavity path including the cQED system and a single-photon pulse is given by

$$\mathcal{H} = \hbar\omega_c a_c^\dagger a_c + \hbar\omega_c |e\rangle_{aa}\langle e| - \hbar\omega_{01} |0\rangle_{aa}\langle 0| \\ + \int_{-\infty}^{\infty} d\omega \hbar\omega a_p^\dagger(\omega) a_p(\omega) + i\hbar g (a_c^\dagger |1\rangle_{aa}\langle e| - a_c |e\rangle_{aa}\langle 1|) \\ + i\hbar \sqrt{\frac{\kappa_{\text{ex}}}{\pi}} \int_{-\infty}^{\infty} d\omega [a_c^\dagger a_p(\omega) - a_p^\dagger(\omega) a_c], \quad (3)$$

where ω_c and ω_{01} are the resonant frequencies of the cavity and the transition of $|0\rangle_a |1\rangle_a$, respectively. System parameters g and κ_{ex} are the atom-cavity coupling constant and the external cavity field decay rate associated with the extraction of the cavity photon to the desired external mode. We also take into account the following dissipative processes: atomic spontaneous emission with a polarization decay rate γ and unwanted cavity field decay due to the imperfection of the cavity with a rate κ_{in} . The total cavity decay rate is given by $\kappa = \kappa_{\text{in}} + \kappa_{\text{ex}}$.

The state of the atom and the photon having horizontal polarization is described as

$$|\psi_H(t)\rangle = |0\rangle_a |0\rangle_c \int_{-\infty}^{\infty} d\omega f_0(t, \omega) a_p^\dagger(\omega) |0\rangle_p \\ + \beta_0(t) |0\rangle_a |1\rangle_c |0\rangle_p \\ + |1\rangle_a |0\rangle_c \int_{-\infty}^{\infty} d\omega f_1(t, \omega) a_p^\dagger(\omega) |0\rangle_p \\ + \beta_1(t) |1\rangle_a |1\rangle_c |0\rangle_p \\ + \beta_e(t) |e\rangle_a |0\rangle_c |0\rangle_p, \quad (4)$$

where ω denotes the frequency of the single-photon pulse, and the functions $f_l(t, \omega)$ ($l \in \{0, 1\}$) and $\beta_m(t)$ ($m \in \{0, 1, e\}$) represent time-dependent probability amplitudes.

Here, we consider the case that the single-photon pulse is nearly resonant with the cavity, and we assume that the atomic state is approximately independent of time. Thus, from the equations of motion of the state $|\psi_H(t)\rangle$ and the input-output relations, we derive response functions in the form of amplitude reflection coefficients, as

$$L_0(\Delta) = \frac{-\kappa_{\text{ex}} + \kappa_{\text{in}} + i\Delta}{\kappa_{\text{ex}} + \kappa_{\text{in}} + i\Delta}, \quad (5)$$

$$L_1(\Delta) = \frac{-\kappa_{\text{ex}} + \kappa_{\text{in}} + i\Delta + g^2/(\gamma + i\Delta)}{\kappa_{\text{ex}} + \kappa_{\text{in}} + i\Delta + g^2/(\gamma + i\Delta)}, \quad (6)$$

where $\Delta \equiv \omega - \omega_c$ is the detuning from the resonant frequency (see Supplemental Material I [19] for the derivation of the response functions).

In a typical one-dimensional cavity setup, g , κ_{in} , and κ_{ex} are described as [2]

$$g = \sqrt{\frac{c\gamma}{2\tilde{A}_{\text{eff}}L_{\text{cav}}}}, \quad (7)$$

$$\kappa_{\text{in}} = \frac{c\alpha_{\text{loss}}}{4L_{\text{cav}}}, \quad (8)$$

$$\kappa_{\text{ex}} = \frac{cT_{\text{ex}}}{4L_{\text{cav}}}, \quad (9)$$

where c , \tilde{A}_{eff} , α_{loss} , T_{ex} , and L_{cav} are the speed of light in vacuum, the effective cavity mode area normalized by a scattering cross-section, the roundtrip loss rate, the coupling mirror transmittance, and the optical length of the cavity, respectively.

We then rewrite Eqs. (5) and (6) using Eqs. (7)-(9) in the form

$$L_0(\Delta) = \frac{-T_{\text{ex}} + \alpha_{\text{loss}} + i4L_{\text{cav}}\Delta/c}{T_{\text{ex}} + \alpha_{\text{loss}} + i4L_{\text{cav}}\Delta/c}, \quad (10)$$

$$L_1(\Delta) = \frac{-T_{\text{ex}} + \alpha_{\text{loss}} + i4L_{\text{cav}}\Delta/c + 2/\left[\tilde{A}_{\text{eff}}(1 + i\Delta/\gamma)\right]}{T_{\text{ex}} + \alpha_{\text{loss}} + i4L_{\text{cav}}\Delta/c + 2/\left[\tilde{A}_{\text{eff}}(1 + i\Delta/\gamma)\right]}. \quad (11)$$

The conditions for an ideal phase flip in the long-pulse limit, i.e., the condition for $L_0 = -1$ and $L_1 = 1$, are derived by substituting $\Delta = 0$ into Eqs. (5) and (6) or Eqs. (10) and (11) as [13]:

$$2C_{\text{in}} \gg \frac{\kappa_{\text{ex}}}{\kappa_{\text{in}}} \gg 1, \quad (12)$$

or

$$\frac{2}{\tilde{A}_{\text{eff}}} \gg T_{\text{ex}} \gg \alpha_{\text{loss}}, \quad (13)$$

where $C_{\text{in}} \equiv g^2/(2\gamma\kappa_{\text{in}}) = 1/(\tilde{A}_{\text{eff}}\alpha_{\text{loss}})$ is an internal cooperativity [14, 15].

To analytically estimate the error probability, we expand the response functions by Δ as

$$L_0(\Delta) = \frac{\alpha_{\text{loss}} - T_{\text{ex}}}{\alpha_{\text{loss}} + T_{\text{ex}}} + i\frac{8L_{\text{cav}}T_{\text{ex}}}{c(\alpha_{\text{loss}} + T_{\text{ex}})^2}\Delta + O(\Delta^2), \quad (14)$$

$$L_1(\Delta) = \frac{\alpha_{\text{loss}} - T_{\text{ex}} + 2/\tilde{A}_{\text{eff}}}{\alpha_{\text{loss}} + T_{\text{ex}} + 2/\tilde{A}_{\text{eff}}} \\ + i\frac{4T_{\text{ex}}(2\tilde{A}_{\text{eff}}L_{\text{cav}}\gamma - c)}{c\gamma(\alpha_{\text{loss}} + T_{\text{ex}} + 2/\tilde{A}_{\text{eff}})^2}\Delta + O(\Delta^2). \quad (15)$$

In both equations, the first terms are real and represent the photon loss, i.e., they contribute to the reduction in the norm of the state function. The second terms are imaginary and describe the pulse delay. A schematic

diagram of the reduction in the norm and the pulse delay is shown in Fig. 2(a).

When an incident pulse is sufficiently long that the terms higher than the second order are negligible (the validity of this approximation and the effect of the higher order terms are discussed later), the photon loss probabilities when the atom is in $|0\rangle_a$ or $|1\rangle_a$ are derived as [12]:

$$l_0 \equiv 1 - L_0(0)^2 = 1 - \left(\frac{\alpha_{\text{loss}} - T_{\text{ex}}}{\alpha_{\text{loss}} + T_{\text{ex}}} \right)^2, \quad (16)$$

$$l_1 \equiv 1 - L_1(0)^2 = 1 - \left(\frac{\alpha_{\text{loss}} - T_{\text{ex}} + 2/\tilde{A}_{\text{eff}}}{\alpha_{\text{loss}} + T_{\text{ex}} + 2/\tilde{A}_{\text{eff}}} \right)^2. \quad (17)$$

These are equivalent to the norm reduction of the states $|0H\rangle$ and $|1H\rangle$, which exist even in the long-pulse limit.

The error due to the photon loss is classified twofold: the reduction in the norm for the total state function, and the unwanted rotation of the state vector due to imbalances in the norm reduction for the bases. The former and latter error probabilities are minimized on the condition of $l_0 + l_1$ and $|l_0 - l_1|$ being minimized, respectively.

As shown in Supplemental Material II [19], the pulse delays for the inputs of the $|0H\rangle$ and $|1H\rangle$ states are given by

$$\tau_0 \equiv \frac{i}{L_0(0)} \left. \frac{dL_0(\Delta)}{d\Delta} \right|_{\Delta=0} = \frac{8L_{\text{cav}}T_{\text{ex}}}{c(T_{\text{ex}}^2 - \alpha_{\text{loss}}^2)}, \quad (18)$$

$$\begin{aligned} \tau_1 &\equiv \frac{i}{L_1(0)} \left. \frac{dL_1(\Delta)}{d\Delta} \right|_{\Delta=0} \\ &= -\frac{T_{\text{ex}}(2\tilde{A}_{\text{eff}}L_{\text{cav}}\gamma - c)}{c\gamma[\alpha_{\text{loss}} + 1/\tilde{A}_{\text{eff}} - \tilde{A}_{\text{eff}}(T_{\text{ex}}^2 - \alpha_{\text{loss}}^2)/4]}. \end{aligned} \quad (19)$$

Figure 2(b) shows the variation of the output pulse delay depending on the input states. These variations cause degradation in the indistinguishability of the photonic qubits, which are experimentally detected as a temporal mode-mismatch error [20]. The gate fidelity reduction due to the pulse delay variation (pulse-delay error) is cancelled by matching the three pulse delays τ_0, τ_1 , and τ_{ref} , where τ_{ref} is the pulse delay of the vertical polarization states from the external mirror. We can minimize the pulse-delay error by minimizing $|\tau_0 - \tau_1|$, as the delay of the pulse from the external mirror τ_{ref} can be freely shifted by adjusting the position of the external mirror. Then, τ_{ref} is set to $\tau_{\text{ref}} = (\tau_0 + \tau_1)/2$ to minimize the pulse-delay error as shown in Fig 2(b).

Based on the formulation of error sources presented above, we derive optimal cavity parameters for the CPF gate. It is known that the norm reduction $l_0 + l_1$ and a measure of the loss imbalance $|l_0 - l_1|$ can be minimized simultaneously by setting the external cavity field decay rate as $\kappa_{\text{ex}} = \kappa_{\text{in}}\sqrt{2C_{\text{in}} + 1}$ [12]. This condition is rewritten using Eqs. (7)-(9) as

$$T_{\text{ex}} = T_{\text{ex}}^{\text{loss}} \equiv \alpha_{\text{loss}} \sqrt{\frac{2}{\tilde{A}_{\text{eff}}\alpha_{\text{loss}}} + 1} \approx \sqrt{\frac{2\alpha_{\text{loss}}}{\tilde{A}_{\text{eff}}}}. \quad (20)$$

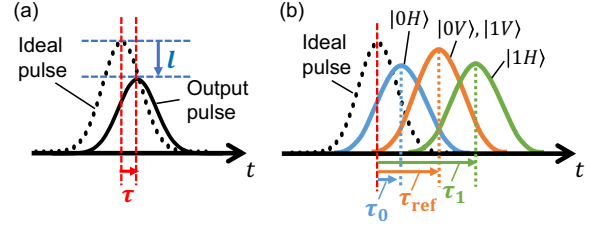


FIG. 2. Schematic of error sources: (a) the loss l and delay τ of the output photon pulse and (b) the output pulse delay depending on the atomic and photonic states and the external mirror position.

For the final approximation, we assume $2C_{\text{in}} \gg 1$, or $2/(\tilde{A}_{\text{eff}}\alpha_{\text{loss}}) \gg 1$ (this approximation is also applied to the following equations). On the other hand, from Eqs. (18) and (19), the condition $\tau_0 = \tau_1$, namely the condition minimizing a measure of the pulse-delay error $|\tau_0 - \tau_1|$, is given by

$$\begin{aligned} T_{\text{ex}} = T_{\text{ex}}^{\text{delay}} &\equiv \sqrt{\frac{8L_{\text{cav}}\gamma}{c} \left(\alpha_{\text{loss}} + \frac{1}{\tilde{A}_{\text{eff}}} \right) + \alpha_{\text{loss}}^2} \\ &\approx \sqrt{\frac{8L_{\text{cav}}\gamma}{c\tilde{A}_{\text{eff}}}}. \end{aligned} \quad (21)$$

Equation (21) is equivalent to $g/\kappa \approx 1$. Figure 3 shows $T_{\text{ex}}^{\text{loss}}$ and $T_{\text{ex}}^{\text{delay}}$ as a function of L_{cav} . As mentioned above, on the curve of $T_{\text{ex}} = T_{\text{ex}}^{\text{delay}}$ (dashed curve), the pulse delay causes no error because $|\tau_0 - \tau_1| = 0$. On the line $T_{\text{ex}} = T_{\text{ex}}^{\text{loss}}$, $l_0 + l_1$ and $|l_0 - l_1|$ are constant as seen in Eqs. (16) and (17). These facts indicate that the total error probability in the CPF gate is minimized at the intersection of the functions, namely $T_{\text{ex}}^{\text{loss}} = T_{\text{ex}}^{\text{delay}}$. From Eqs. (20) and (21), we obtain the optimal cavity length

$$L_{\text{cav}}^{\text{opt}} = \frac{c}{4\gamma(\tilde{A}_{\text{eff}} + \alpha_{\text{loss}}^{-1})} \approx \frac{c\alpha_{\text{loss}}}{4\gamma}. \quad (22)$$

Note that Eq. (22) can be rewritten as $\kappa_{\text{in}} \approx \gamma$. In other words, adjusting the cavity length to balance the internal-loss rate and the atomic polarization decay rate minimizes the total error probability. For reference, typical experimental parameters are shown: $\kappa_{\text{in}}/\gamma = 0.067$ in a free-space cavity [6], $\kappa_{\text{in}}/\gamma = 8.3$ in a fiber cavity [21], $\kappa_{\text{in}}/\gamma = 460$ in a nanophotonic cavity [22], and $\kappa_{\text{in}}/\gamma = 0.04$ in a nanofiber cavity [13, 23]. These values suggest that these typical cavity systems are required to be adjusted significantly for cQED-based quantum computing.

In the above discussion, we have assumed that the dependence of \tilde{A}_{eff} and α_{loss} on the cavity length is negligible. This is justified in typical optical cavities, where the bulk loss of photons (due to absorption and scattering in the cavity medium) is negligible. On the other hand, in some systems, including photonic crystal cavities, the

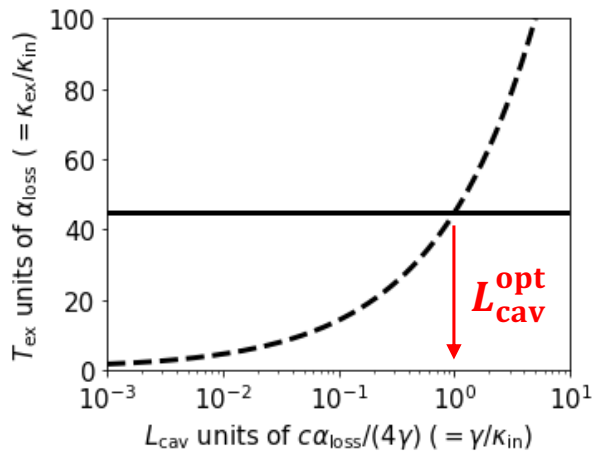


FIG. 3. Transmittance minimizing the photon loss probability $T_{\text{ex}} = T_{\text{ex}}^{\text{loss}}$ in Eq. (20) (solid line) and the transmittance minimizing the pulse-delay error rate $T_{\text{ex}} = T_{\text{ex}}^{\text{delay}}$ in Eq. (21) (dashed curve), as a function of the cavity length L_{cav} . They intersect at optimal cavity length $L_{\text{cav}} = L_{\text{cav}}^{\text{opt}}$. These plots are calculated by setting the internal cooperativity to $C_{\text{in}} = 1000$. We assume that α_{loss} is independent of L_{cav} .

bulk loss cannot be neglected [16–18]. For example, they have roundtrip loss α_{loss} depending on cavity length as $\alpha_{\text{loss}} = 1 - \exp[-(\alpha' + \beta L_{\text{cav}})] \approx \alpha' + \beta L_{\text{cav}}$, where the approximation holds when $\alpha_{\text{loss}} \ll 1$. The first term mainly comes from the scattering of cavity mirrors, and the other mainly comes from bulk loss. Solving Eq. (22) again for L_{cav} , we obtain the optimal cavity length considering the bulk loss

$$L_{\text{cav}}^{\text{bulk}} \approx \frac{c\alpha'}{4\gamma - c\beta}. \quad (23)$$

This result indicates that the photon loss coefficient of the cavity length dependence β should be less than $4\gamma/c$ for the existence of the optimal cavity length. In other words, if the bulk loss is dominant, a cavity length of 0 is optimal.

Here, we discuss the shift of the optimal cavity length due to the effect of the pulse distortion represented by the higher order terms in Eqs. (14) and (15) by solving Eqs. (A1)–(A5) numerically. We consider an input photon wave packet having a Gaussian shape as $f^{\text{in}}(t) = \sqrt{\frac{1}{\sqrt{\pi}W_t}} \exp\left(-\frac{t^2}{2W_t^2}\right)$, where W_t represents the pulse duration [24].

To estimate the total error of the CPF gate operation, we calculate a gate fidelity F defined by

$$F = |\langle \Psi_{\text{id}} | \Psi_{\text{out}} \rangle|^2, \quad (24)$$

where $|\Psi_{\text{id}}\rangle$ is the output state when the ideal CPF gate operation would be achieved. In the numerical calculation, the initial states of the atomic and photonic qubits are set to $\alpha_0 = \alpha_1 = \alpha_{\text{H}} = \alpha_{\text{V}} = 1/\sqrt{2}$ to average F over all initial conditions [13].

Figure 4(a) shows the fidelity F as a function of the Gaussian pulse duration W_t and the cavity length L_{cav} . The red solid line denotes the cavity length in Eq. (22), and the blue dashed curve denotes the cavity length maximizing F calculated numerically for each pulse duration. They are in very good agreement for $W_t \gtrsim 0.1\gamma^{-1}$.

For $W_t \lesssim 0.1\gamma^{-1}$, on the other hand, there is a discrepancy between the red solid line and blue dashed curve due to the effect of the higher-order terms of Δ in Eqs. (14) and (15). The condition of the pulse duration where the higher order terms can be considered negligible, that is, the pulse duration at the branch of the red solid line and the blue dashed curve in Fig. 4(a), can be roughly estimated from the point where the values of the first and second terms in Eqs. (14) and (15) are equal. From the discussion in Supplemental Material III [19], this condition can be written as $W_t \gg \max(1/\kappa, \kappa/g^2)$ when the cavity length is optimal as shown in Eq. (22) or (23). Then, using Eqs. (12) and (20), we obtain the pulse duration condition where the first-order approximation is valid as

$$W_t \gg \max\left(\frac{1}{\kappa}, \frac{\kappa}{g^2}\right) \approx \frac{1}{\gamma\sqrt{2C_{\text{in}}}}. \quad (25)$$

When the second-order or higher terms are raised, the fidelity remarkably drops. Then, the pulse duration should be at least as long as the right-hand side of Eq. (25), indicated by the red star in Fig. 4(a). We note that the speed of the CPF gate is characterized by the right-hand side of Eq. (25), determined by C_{in} and γ under the optimal cavity condition.

Figure 4(b) shows the result of the coupling rate g/κ for the same simulation as Fig 4(a). From Fig. 4(b), we can obtain a hint regarding the optimal cavity design even when the first-order approximation is invalid. The fact that the numerically optimized L_{cav} (blue dashed curve) is in good agreement with $g/\kappa = 1$ (white region) suggests that the condition for minimizing the temporal mode-mismatch error, i.e., $\tau_0 = \tau_1$ or Eq. (21), holds even for $W_t \lesssim 0.1\gamma^{-1}$. In other words, $T_{\text{ex}}^{\text{loss}}$ in Eq. (20) is no longer valid, even though $T_{\text{ex}}^{\text{delay}}$ in Eq. (21) is still valid in this region. Thus, the optimal cavity length becomes shorter than that in Eq. (22) [or Eq. (23)] for such short pulses. This argument is supported by the discussion in Supplemental Material IV [19], where we show that the higher-order term effect is corrected by decreasing L_{cav} .

We have investigated the optimal cavity parameters for cQED-based CPF gates with photons having finite pulse duration. From the response function of the cQED system, we formulated two error sources: the photon loss probability and the error rate due to temporal mode-mismatch of the output photon pulse, which we take into account as pulse delay. We then derived the optimal condition of the tunable cavity parameters. As a result, the balance of the photonic and atomic decay rate ($\kappa_{\text{in}} = \gamma$) was derived for optimization of the cavity length. Furthermore, we performed a numerical simulation of the dynamics of the cQED system for fast gate operations

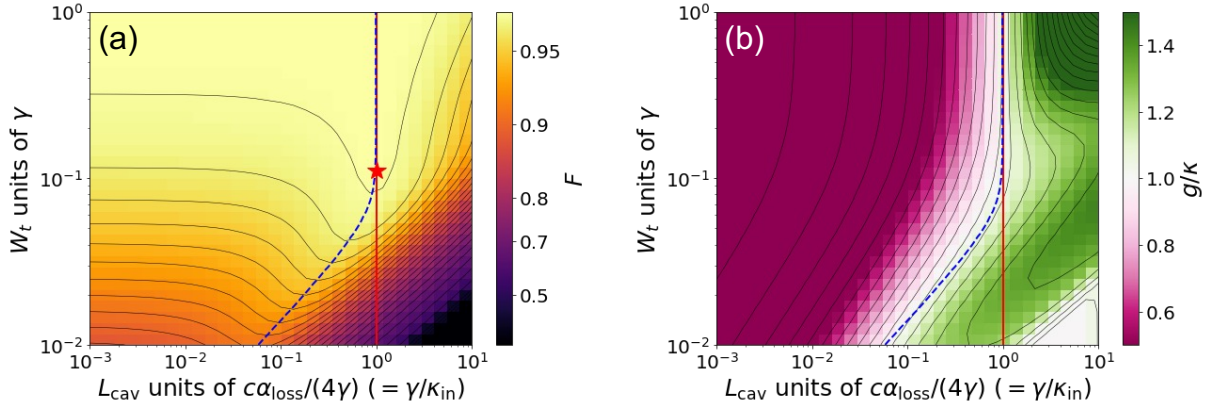


FIG. 4. (a) Simulation result of the fidelity F as a function of W_t and L_{cav} when T_{ex} is optimized numerically. The red solid line represents $L_{\text{cav}} = L_{\text{cav}}^{\text{opt}}$ in Eq. (22), and the blue dashed curve represents the cavity length optimized numerically for each pulse duration. The red star represents five times the right-hand side of Eq. (25), that is, $W_t = 5/(\gamma\sqrt{2C_{\text{in}}})$. The pulse delay of the photon reflecting the external mirror is set to $\tau_{\text{ref}} = (\tau_0 + \tau_1)/2$, and the internal cooperativity is set to $C_{\text{in}} = 1000$. (b) The coupling rate in the same simulation of (a). The optimized cavity length (blue dashed curve) and $g/\kappa = 1$ region are in good agreement for any pulse duration.

where temporal mode-mismatch errors beyond the first-order approximation are not negligible. However, in such a regime, error probabilities in the CPF gate are quite high (over five percent), indicating that our optimal cavity design obtained analytically is basically valid for the purpose of scalable quantum computing.

Regarding future work, a similar argument should be valid for other cQED-based entangling gates [2]. We note that the optimal cavity parameters and pulse duration condition for CPF gates derived in this work are consistent for single-photon generation [25]. Thus, it is possible to realize both single-photon generation and the CPF gate using the same cQED setup, which appears to be efficient for the construction of cQED-based quantum computing systems.

ACKNOWLEDGEMENT

The authors thank Hayato Goto, Rina Kanamoto, Samuel Ruddell, Karen Webb, and Akinori Suenaga for their helpful comments. This work was supported by JST CREST, Grant Number JPMJCR1771, and JST Moonshot R&D, Grant Number JPMJMS2061, Japan.

SUPPLEMENTAL MATERIAL

I. DERIVATION OF $L_0(\Delta)$ AND $L_1(\Delta)$

Phenomenologically introducing the internal cavity field decay rate κ_{in} , the total cavity field decay rate $\kappa = \kappa_{\text{in}} + \kappa_{\text{ex}}$, and the atomic polarization decay rate γ , we obtain the equations of motion by using Eqs. (3) and

(4) in the main text as [11, 12]

$$\dot{B}_0(t) = -\kappa B_0(t) - \sqrt{\frac{\kappa_{\text{ex}}}{\pi}} \int_{-\infty}^{\infty} d\omega F_0^{\text{in}}(x=0) e^{-i\omega t}, \quad (26)$$

$$\dot{B}_1(t) = g B_e(t) - \kappa B_1(t) - \sqrt{\frac{\kappa_{\text{ex}}}{\pi}} \int_{-\infty}^{\infty} d\omega F_1^{\text{in}}(x=0) e^{-i\omega t}, \quad (27)$$

$$\dot{B}_e(t) = -g B_1(t) - \gamma B_e(t), \quad (28)$$

$$F_0^{\text{out}}(x=0) = F_0^{\text{in}}(x=0) + \sqrt{\frac{\kappa_{\text{ex}}}{\pi}} \int_0^t dt' B_0 e^{-i\omega t'}, \quad (29)$$

$$F_1^{\text{out}}(x=0) = F_1^{\text{in}}(x=0) + \sqrt{\frac{\kappa_{\text{ex}}}{\pi}} \int_0^t dt' B_1 e^{-i\omega t'}, \quad (30)$$

where

$$B_0(t) = e^{i(\omega_c - \omega_{01})t} \beta_0(t), \quad (31)$$

$$B_1(t) = e^{i\omega_c t} \beta_1(t), \quad (32)$$

$$B_e(t) = e^{i\omega_c t} \beta_e(t), \quad (33)$$

$$F_0^{\text{in}}(x=0) = -f_0(\omega, t=0) e^{i(\omega_c - \omega_{01})t}, \quad (34)$$

$$F_1^{\text{in}}(x=0) = -f_1(\omega, t=0) e^{i\omega_c t}, \quad (35)$$

$$F_0^{\text{out}}(x=0) = -f_0(\omega, t) e^{i(\omega_c - \omega_{01})t}, \quad (36)$$

$$F_1^{\text{out}}(x=0) = -f_1(\omega, t) e^{i\omega_c t}. \quad (37)$$

In deriving above equations, we used $\int_0^t \beta_m(t') \delta(t-t') dt' = \beta_m(t)/2$ ($m \in \{0, 1, e\}$). Global phases are neglected in Eqs. (29) and (30). Assuming sufficiently long pulses, we perform the approximations $\dot{B}_0(t) \simeq 0$, $\dot{B}_1(t) \simeq 0$ and $\dot{B}_e(t) \simeq 0$. Then, we obtain $L_0(\Delta)$ and $L_1(\Delta)$ in Eqs. (5) and (6) in the main text [12].

II. DERIVATION OF PULSE DELAY

Here, we show that l_n and τ_n ($n \in \{0, 1\}$) defined by Eqs. (16)-(19) in the main text represent the photon loss probabilities and the pulse delays, respectively. The functions $L_n(\Delta)$ ($n \in \{0, 1\}$) in Eqs. (5) and (6) in the main text are expanded by

$$L_n(\Delta) = L_n(0) + \left. \frac{dL_n(\Delta)}{d\Delta} \right|_{\Delta=0} \Delta + O(\Delta^2). \quad (38)$$

When Δ is sufficiently small, this becomes

$$L_n(\Delta) \approx L_n(0) \exp \left[\left. \frac{1}{L_n(0)} \frac{dL_n(\Delta)}{d\Delta} \right|_{\Delta=0} \Delta \right]. \quad (39)$$

Comparing Eq. (38) and Eqs. (14) and (15) in the main text, we find that the first term of Eq. (38) is real ($L_n(0) \in \mathbb{R}$) and the second term of Eq. (38) is imaginary ($\left. \frac{dL_n(\Delta)}{d\Delta} \right|_{\Delta=0} \in \mathbb{I}$), thus, the inside of the exponential function in Eq. (39) is imaginary. Then, Eq. (39) is rewritten by

$$L_n(\Delta) \approx L_n(0) \exp(-i\Delta\tau_n). \quad (40)$$

where we used the relation $-i\tau_n = \left. \frac{1}{L_n(0)} \frac{dL_n(\Delta)}{d\Delta} \right|_{\Delta=0}$ ($n \in \{0, 1\}$) introduced by Eqs. (18) and (19) in the main text. From the time shifting property of a Fourier transform \mathbf{F} on a pulse waveform $f_n(t)$ ($n \in \{0, 1\}$),

$$\mathbf{F}[f_n(t - \tau_n)](\Delta) = \mathbf{F}[f_n(t)] \exp(-i\Delta\tau_n), \quad (41)$$

we obtain the output pulse waveform $f_n^{\text{out}}(t)$ ($n \in \{0, 1\}$) as

$$\begin{aligned} f_n^{\text{out}}(t) &= \mathbf{F}^{-1} \{ \mathbf{F}[f_n(t)](\Delta) L_n(\Delta) \} \\ &= L_n(0) \mathbf{F}^{-1} \{ \mathbf{F}[f_n(t)](\Delta) \exp(-i\Delta\tau_n) \} \\ &= L_n(0) f(t - \tau_n). \end{aligned} \quad (42)$$

Equation (42) shows that the output pulse is multiplied by $L_n(0)$, i.e., the photon loss probabilities can be represented by $l_n \equiv 1 - L_n(0)^2$ and the output pulse is delayed to τ_n .

III. CONDITION FOR THE FIRST ORDER APPROXIMATION

We expand Eq. (6) in the main text by Δ as

$$\begin{aligned} L_1(\Delta) &= \left(1 - \frac{2\gamma\kappa_{\text{ex}}}{g^2 + \gamma\kappa} \right) \\ &- i \frac{2\kappa_{\text{ex}}(g^2 - \gamma^2)}{(g^2 + \gamma\kappa)^2} \Delta - \frac{2\kappa_{\text{ex}}(2g^2\gamma + g^2\kappa - \gamma^3)}{(g^2 + \gamma\kappa)^3} \Delta^2 + O(\Delta^3). \end{aligned} \quad (43)$$

Thus, the condition that the higher order terms above second order are negligible is

$$\left| \frac{2\kappa_{\text{ex}}(g^2 - \gamma^2)}{(g^2 + \gamma\kappa)^2} \right| \Delta \gg \left| \frac{2\kappa_{\text{ex}}(2g^2\gamma + g^2\kappa - \gamma^3)}{(g^2 + \gamma\kappa)^3} \right| \Delta^2 \quad (44)$$

$$\rightarrow \Delta \ll \frac{(g^2 - \gamma^2)(g^2 + \gamma\kappa)}{2g^2\gamma + g^2\kappa - \gamma^3} \approx \frac{g^2}{\kappa}, \quad (45)$$

where the approximation in the second line holds when $g \approx \kappa \gg \gamma \approx \kappa_{\text{in}}$ [the optimal condition as shown in Eqs. (12), (21), (22), and (23) in the main text] is satisfied.

When $g = 0$, we obtain the condition for $L_0(\Delta)$ as

$$\Delta \ll \kappa. \quad (46)$$

Since the condition $\Delta \ll \Delta_c$ means that the pulse duration W_t is required to be sufficiently longer than $1/\Delta_c$, we finally obtain the condition on the pulse duration for the first order approximation, $W_t \gg \max(1/\kappa, \kappa/g^2)$.

IV. EFFECT OF HIGHER-ORDER TERMS

We show that the higher-order term effect is corrected by decreasing L_{cav} . First, we consider the optimization of T_{ex} for a certain cavity length. When the pulse duration is so short that the second-order term of Δ is not negligible, as shown in Fig. 5, $l_0(\Delta) = 1 - |L_0(\Delta)|^2$ decreases and $l_1(\Delta) = 1 - |L_1(\Delta)|^2$ increases as $|\Delta|$ increases. On the other hand, $\tau_0(\Delta) = \left| \frac{d}{d\Delta} \arg L_0(\Delta) \right|$ decreases and $\tau_1(\Delta) = \left| \frac{d}{d\Delta} \arg L_1(\Delta) \right|$ increases as $|\Delta|$ increases. Therefore, T_{ex} needs to be optimized to compensate for this effect. The first derivatives of the photon loss probabilities and the pulse delays for T_{ex} are given by

$$\frac{dl_0}{dT_{\text{ex}}} = -\frac{4\alpha_{\text{loss}}(T_{\text{ex}} - \alpha_{\text{loss}})}{(T_{\text{ex}} + \alpha_{\text{loss}})^3} < 0, \quad (47)$$

$$\frac{dl_1}{dT_{\text{ex}}} = \frac{4(2/\tilde{A}_{\text{eff}} + \alpha_{\text{loss}})(2/\tilde{A}_{\text{eff}} - T_{\text{ex}} + \alpha_{\text{loss}})}{(2/\tilde{A}_{\text{eff}} + T_{\text{ex}} + \alpha_{\text{loss}})^3} > 0, \quad (48)$$

$$\frac{d\tau_0}{dT_{\text{ex}}} = -\frac{8L_{\text{cav}}(T_{\text{ex}}^2 + \alpha_{\text{loss}}^2)}{c(T_{\text{ex}}^2 - \alpha_{\text{loss}}^2)^2} < 0, \quad (49)$$

$$\begin{aligned} \frac{d\tau_1}{dT_{\text{ex}}} &= \frac{4(c/\tilde{A}_{\text{eff}} - 2L_{\text{cav}}\gamma)(T_{\text{ex}}^2 + \alpha_{\text{loss}}^2 + 4\alpha_{\text{loss}}/\tilde{A}_{\text{eff}} + 4/\tilde{A}_{\text{eff}}^2)}{c\gamma(T_{\text{ex}} - \alpha_{\text{loss}} - 2/\tilde{A}_{\text{eff}})^2(T_{\text{ex}} + \alpha_{\text{loss}} + 2/\tilde{A}_{\text{eff}})^2} \\ &> 0, \end{aligned} \quad (50)$$

where we used the relation of Eq. (13) in the main text at each inequality and $L_{\text{cav}} \approx L_{\text{cav}}^{\text{opt}} \approx c\alpha_{\text{loss}}/(4\gamma)$ in the inequality of Eq. (D4). From Eqs. (D1)-(D4), it is expected that a smaller value of T_{ex} than that obtained using the first-order approximation is optimal for the CPF gate when considering the higher-order terms. Thus, the optimal cavity length becomes shorter than that in Eq. (22) [or Eq. (23)] in the main text because $T_{\text{ex}} \propto \sqrt{L_{\text{cav}}}$ [see Eq. (21)]. Thus for short pulses, and therefore for fast gate operations, the temporal mode-mismatch errors beyond the first-order approximation are not negligible.

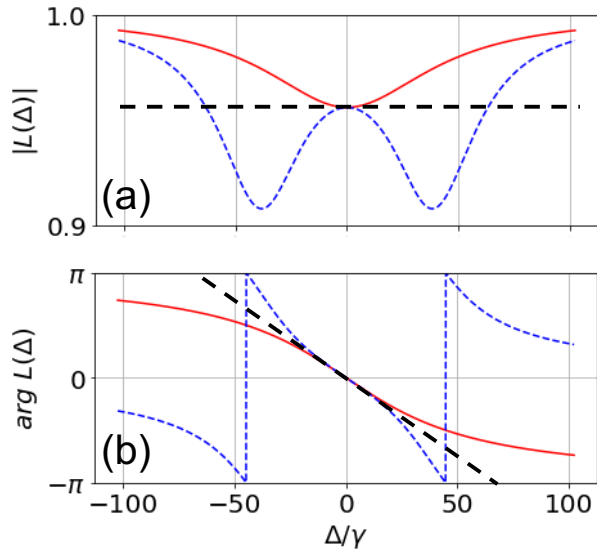


FIG. 5. The plot of amplitude reflection coefficients: (a) amplitudes and (b) phases of $L_0(\Delta)$ (red solid curve) and $L_1(\Delta)$ (blue dashed curve) in the case of $\kappa_{\text{in}} = \gamma$ and $T_{\text{ex}} = T_{\text{ex}}^{\text{loss}} = T_{\text{ex}}^{\text{delay}}$. The black dashed lines represent a first-order approximation of amplitude and phase. The phase of $L_0(\Delta)$ is shifted by π from the original value. The system parameters are set to $(\kappa_{\text{in}}/\gamma, C_{\text{in}}) = (1, 1000)$.

-
- [1] M. A. Nielsen and I. Chuang, *Quantum Computation and Quantum Information* (Cambridge University Press, 2000).
- [2] A. Reiserer and G. Rempe, *Rev. Mod. Phys.* **87**(4), 1379 (2015).
- [3] Y. F. Xiao, Z. F. Han, Y. Yang, and G. C. Guo, *Phys. Lett. A* **330**(3), 137 (2004).
- [4] L. M. Duan, B. Wang, and H. J. Kimble, *Phys. Rev. A* **72**, 032333 (2005).
- [5] S. Welte, B. Hacker, S. Daiss, S. Ritter, and G. Rempe, *Phys. Rev. X* **8**, 011018 (2018).
- [6] S. Daiss, S. Langenfeld, S. Welte, E. Distanto, P. Thomas, L. Hartung, O. Morin, and G. Rempe, *Science* **371**(6529), 614 (2021).
- [7] L. M. Duan and H. J. Kimble, *Phys. Rev. Lett.* **92**(12), 127902 (2004).
- [8] B. Hacker, S. Welte, G. Rempe, and S. Ritter, *Nature* **536**(7615), 193 (2016).
- [9] A. Reiserer, N. Kalb, G. Rempe, and S. Ritter, *Nature* **508**(7495), 237 (2014).
- [10] T. G. Tiecke, J. D. Thompson, N. P. Leon, L. R. Liu, V. Vuletić, and M. D. Lukin, *Nature* **508**(7495), 241 (2014).
- [11] H. Goto and K. Ichimura, *Phys. Rev. A* **72**, 054301 (2005).
- [12] H. Goto and K. Ichimura, *Phys. Rev. A* **82**, 032311 (2010).
- [13] R. Asaoka, Y. Tokunaga, R. Kanamoto, H. Goto, and T. Aoki, *Phys. Rev. A* **104**(4), 043702 (2021).
- [14] S. Rosenblum, O. Bechler, I. Shomroni, Y. Lovsky, G. Guendelman, and B. Dayan, *Nat. Photon.* **10**(1), 19 (2016).
- [15] H. Goto, S. Mizukami, Y. Tokunaga, and T. Aoki, *Phys. Rev. A* **99**(5), 053843 (2019).
- [16] K. J. Vahala, *Nature* **424**(6950), 839 (2003).
- [17] A. V. Kavokin, J. J. Baumberg, G. Malpuech, and F. P. Laussy, *Microcavities* (Oxford university press, 2017).
- [18] D. E. Chang, J. S. Douglas, A. G. Tudela, C. L. Hung, and H. J. Kimble, *Rev. Mod. Phys.* **90**(3), 031002 (2018).
- [19] See Supplemental Material
- [20] P. P. Rohde, T. C. Ralph, and M. A. Nielsen, *Phys. Rev. A* **72**(5), 052332 (2005).
- [21] T. Macha, E. Uruñuela, W. Alt, M. Ammenwerth, D. Pandey, H. Pfeifer, and D. Meschede, *Phys. Rev. A* **101**(5), 053406 (2020).
- [22] P. Samutpraphoot, T. Dordevic, P. L. Ocola, H. Bernien, C. Senko, V. Vuletic, and M. D. Lukin, *Phys. Rev. Lett.* **124**(6), 063602 (2020).
- [23] S. K. Ruddell, K. E. Webb, M. Takahata, S. Kato, and T. Aoki, *Opt. Lett.* **45**(17), 4875 (2020).
- [24] A Gaussian pulse is one suitable waveform for fast quantum gates due to its tolerance against the effects of mode-mismatch due to pulse delay (i.e., a pair of Gaussian pulses with a certain shift has a larger overlapping integral than a pair of any other functions with the same shift and the same bandwidth) [20]. In addition, several previous studies have suggested that a single-photon source based on cQED with a three-level atom can precisely control the standard deviation of an emitted Gaussian pulse [25–28].

- [25] T. Utsugi, A. Goban, Y. Tokunaga, H. Goto, and T. Aoki, *Phys. Rev. A* **106**(2), 023712 (2022).
- [26] G. S. Vasilev, D. Ljunggren, and A. Kuhn, *New Journal of Physics* **12**(6), 063024 (2010).
- [27] A. Kuhn and D. Ljunggren, *Contemporary Physics* **51**(4), 289 (2010).
- [28] P. B. Nisbet-Jones, J. Dille, D. Ljunggren, and A. Kuhn, *New Journal of Physics* **13**(10), 103036 (2011).